Process refinement through Design of Experiments (Taguchi) to reduce porosity levels of thin Flame Spray NiCrBSi coatings on cast Aluminium alloys

David Culliton, Dept. Mechanical Eng., Dublin Institute of Technology, Bolton St., Dublin

David Kennedy, Dept. Mechanical Eng., Dublin Institute of Technology, Bolton St., Dublin

Anthony Betts, Dept. Research and Enterprise and Applied Electrochemistry Group, Focas, Dublin Institute of Technology, Rathmines Rd., Dublin

Abstract

Thin(<100µm) NiCrBSi Flame Spray Coatings were applied to two cast aluminium alloys, high-copper LM24 and low-copper LM25. A Taguchi full factorial design of experiments L_{16} matrix of key deposition parameters was constructed to develop the optimum spray parameters. The effects of parameter variations on the porosity levels of these coatings were assessed. Key parameter interactions were reported. Quantifiable interactions between the selected parameters were noted for the LM24 substrate. However, on the LM25 substrate these interactions were much less defined. Corrosion performance of the optimised coatings, based on electrochemical impedance spectroscopy, was reported. The presence of through-pores in the coatings were shown to reduce the corrosion resistance of the coated systems by a factor of 10, in dilute NaCl solutions, compared to bulk 316L stainless steel.

1 Introduction

Flame Spraying was originally invented by Max Ulrich Schoop in the early 1900s and was initially used for the application of zinc[1]. In the 1930s its use was expanded to include the application of hard bearing coatings onto steel balls and its applicability was further enhanced throug the 1950s and beyond as new materials became available. It is still widely used today as a low-cost Thermal Spray process. However, the concern with coatings deposited with the Flame Spray system centres around oxidation of the in-flight particles and the development of porosity in the coating. This is related to the low particle velocity (<150m·s^{-1}) which necessitates the powder particles being molten prior to deposition. These coating defects become even more important when attempting to apply a thin porosity-free coating, particularly in corrosion-resistance applications.

Work done by Stokes et al[2] have concluded that low-porosity coatings may be achieved by controlling the spraying temperature. It was found by Guilemany et al[3] that spraying distance also has a crucial role to play in the resultant corrosion resistance of the coatings, particularly

in the presence of hydrogen. This can be attributed to poor flattening of the particles or splats. In work by Kawakita et al[4] it was noted that degradation of the pores in the coatings proceeded in a manner similar to crevice corrosion and that it depended on the number of pores and the sensitivity of the coating material to the active environment. In addition, if the coating had no penetrating path(no through-pores), the corrosion resistance of the coated substrate depended on the corrosion resistance of the coating itself, and that to avoid these through-pores necessitated the production of denser, less oxidised coatings. These coatings, it was shown, required higher velocity and lower temperature of the sprayed particles. The incompatibility of these requirements was overcome by using an inert gas shroud. The design concept was based on the flame being surrounded by the high flow rate inert gas. This enabled increased particle in-flight speeds and a molten fraction below 40%.

Work carried out by Hanson et al[5] found similar results when these two factors were controlled independently. However, in studies by Fukushima et al[6] on the oxidation of Thermal Sprayed 316L SS coatings, it was found that a reduction of spray distance significantly increased the oxygen level due to the excessive heating of substrates by the flame. It was revealed that when a nitrogen-gas shield was incorporated into the design, the oxidation during flight was around 0.2 wt% and oxide levels in the coating were measured below 0.15 wt%. However, coating porosity increased from 0.5 to 2.5 vol%. In work by Kuroda et al[7] the level of oxidation was reduced to 0.19wt.% by changing the composition of the combustion gas, in conjunction with a gas shroud. However, further reductions of the oxygen content resulted in an increase in the porosity of the coating. This may have been related to a lowering of the particle temperature due to the presence of the nitrogen. The authors reported that, by controlling the nitrogen/oxygen mix, porosity and oxide reductions were achieved.

In summary it may be stated that porosity is affected by:

- Particle velocity
- Particle temperature
- Spraying Distance
- Oxidation levels

The aim of this work was to investigate the effect of deposition process parameters on the porosity levels of thin (≤100μm) Flame Spray Thermal Spray coatings when applied to two

cast aluminium alloys[8] - LM24(high Cu content, high hardness) and LM25(low Cu-content, low hardness). In order to achieve this, a Taguchi Full Factorial L_{16} Design of Experiments approach was developed.

The main objectives of this work were:

1.1 To refine the coating application technique and to reduce porosity and in-flight particle oxidation.

1.2 To identify key interactions between process parameters

1.3 To gain insight into and an understanding of corrosion performance mechanisms.

2 Experimental

Prior to application of the Thermal Spray coatings, all panels were cleaned by grit blasting using a Guyson manual grit blasting machine and white alumina grit, followed by 5 minutes immersion in acetone in an ultrasonic bath.

2.1 Coating Application

Coatings were applied using two different application systems. Two as-cast Al-alloys were investigated : LM24 and LM25. The main compositional constituents are given in Table 1.

	Nominal Composition (wt.%)									
Alloy	Al	Si	Fe	Cu	Mn	Mg	Zn	Ni	Cr	B
LM24	86.0	8.92	1.00	2.11	0.20	0.18	1.13	0.06	0.04	-
LM25	92.2	6.53	0.45	0.06	0.10	0.28	0.06	<0.01	0.02	-
NiCrBSi	-	4-4.5	2.75	-	-	-	-	(Base)	15-17	3-3.4

Table 1 Composition of aluminium alloys and the NiCrBSi Flame Spray coating.

Parameters and settings are shown in Table 2. For the Castolin Eutectic Castodyn 8000 system, control of gas flow is based on gas pressures, similar to the Oxy-Acetylene welding process. In addition the system has 4 different nozzle types, which are designed for the application of specific materials. In the case of cermet and metallic coatings, the manufacturer recommends either nozzle 1 or nozzle 2. Powder flow rate is controlled by a 5 setting with system. Manufacturers recommendations suggest that the optimum settings are either 2 or 3. Gas flow rates were set at the recommended 0.05 MPa (Acetylene) and 0.45 MPa (Oxygen). For additional particle speed, compressed air is often included as a carrier

gas. In this project it was decided to replace the compressed air with argon, in an attempt to provide some level of shielding for the in-flight particles, in order to reduce in-flight oxidation[9,10]. Initial trials with argon indicated that flow rates of 9 and 14 normal litres per minute (nlpm) were optimum. Nominal coating thickness was 100µm.

Parameter		**Setting**	
		Low	High
Nozzle	**Type**	1	2
	Distance (mm)	200	300
Argon (nlpm) [MFR_g]		9	14
Powder Flow Rate ($kg \cdot h^{-1}$) [MFR_P]		2	3

Table 2 Parameters for the Flame Spray DOE work.

Run configurations were based on a Taguchi Multi-Factorial L_{16} Design, as shown in Table 3.

Run	**Nozzle**		**MFR_g** (nlpm)	**MFR_P** ($kg \cdot h^{-1}$)
	Type	**Distance** (mm)		
R01	1 (20)	300	9	2
R02	2 (10)	200	9	3
R03	1 (20)	200	14	3
R04	1 (20)	300	9	3
R05	2 (10)	300	9	2
R06	1 (20)	300	14	2
R07	2 (10)	300	14	3
R08	2 (10)	200	14	3
R09	1 (20)	200	9	3
R10	2 (10)	300	9	3
R11	1 (20)	200	9	2
R12	1 (20)	200	14	2
R13	1 (20)	300	14	3
R14	2 (10)	200	9	2
R15	2 (10)	200	14	2
R16	2 (10)	300	14	2

Table 3 DoE design for the FS coatings

2.2 Microstructural Analysis

Samples were sectioned, mounted, ground and polished to characterise the substrate, coating and interface. Samples (1cm^2) were mounted in an Epomet F resin using a Buehler SimpliMet® 3000 Automatic Mounting Press**.** The heating/cooling process was 8min/4min, respectively. Grinding was performed on a Buehler Metaserv automatic grinder/polisher, as per Table 3, with pro-rotation at 200rpm and a constant load of approximately 400N.

Step			Time(min)
1	SiC Paper	240 Grit	3.5
2		600 Grit	3.5
3		800 Grit	3.5
4		1200 Grit	3.5
5	Diamond Paste / Microcloth	9 µm	3.0
6		6 µm	3.0
7		3 µm	3.0
8	Final Polishing	0.05 µm	3.0

Table 4 Grinding and Polishing Steps

Pressure-mounting EPOMET® F is a thermosetting epoxy resin with high hardness, good chemical resistance and has finer grains designed to penetrate the smallest cracks and features. The higher hardness, whilst retaining the ability to better profile the coating dramatically reduces the incidence of grain pull-out[11] during grinding/polishing processes.

Microstructural analysis was performed on a Reichert-Jung Me3 metallurgical microscope and an Olympus BX60M metallurgical microscope. Metallographic analysis, coating thickness measurements and porosity measurements were performed, using image analysis software.

2.3 Taguchi Analysis

Results of the porosity and coating thickness measurements were used to analyse the effect of the deposition parameters. Both singular and interactive effects were studied, using the Design8Ease package, version 8.0.5.

2.4 CorrosionAnalysis

Short Term Corrosion testing was performed using the Electrochemical Spectroscopy (EIS) technique. This is a three-electrode technique, consisting of a Reference Electrode (Ag/AgCl, sat.KCl), a Counter Electrode (Pt) and a Working Electrode (samples). A schematic of the configuration is shown in Figure 1.

EIS testing was performed in a 0.1M NaCl solution. The selection of this molarity was based on the published work by Seri[12] who found that the extent of dissolution around intermetallic

particles, in aluminium alloys, depended on NaCl concentrations and that dilute NaCl solutions (0.01-0.1 M) resulted in greatest dissolution of the aluminium matrix. System configuration for all tests in 0.1M NaCl was 10mV perturbation, Frequency Range 10^{6} to 10^{-2} with 10 points per interval.

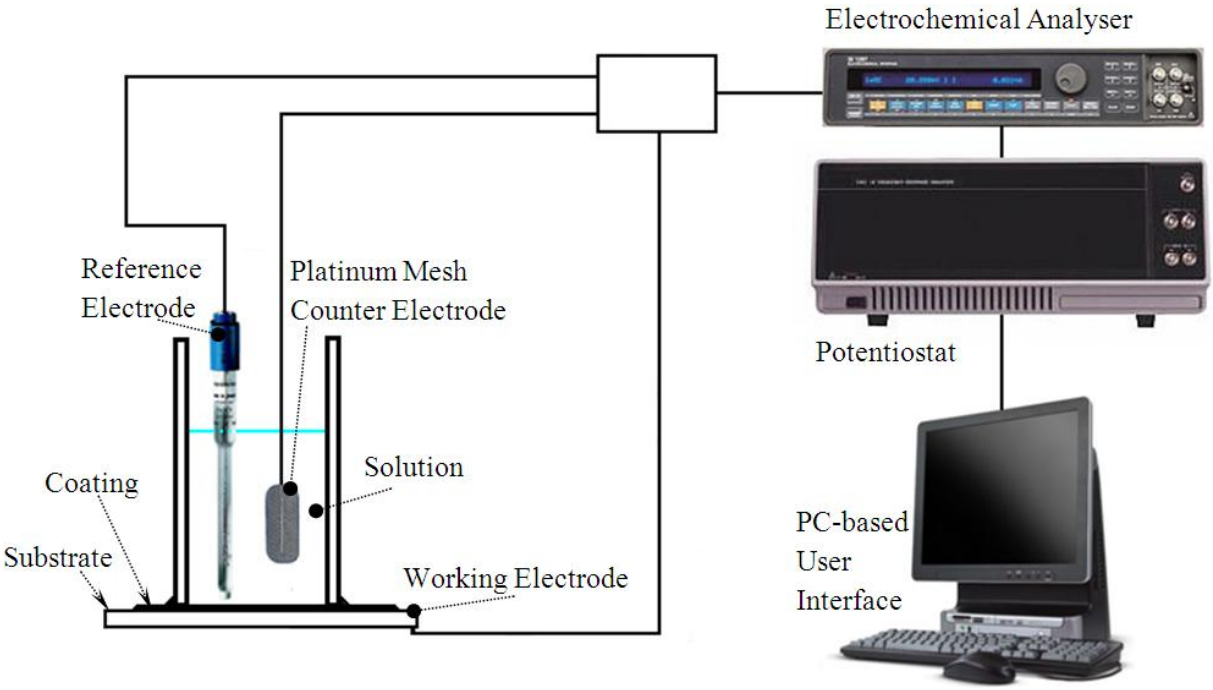

Figure 1 Schematic of the setup for electrochemical corrosion testing (EIS)

3 Results and discussion

3.1 Microstructural Analysis

Coated samples were subjected to microstructural analysis to characterise the coatings and determine coating porosity levels. Sample micrographs are provided in Figure 2. Large variations in coating integrity were noted for the coated samples. In generally the coatings were defined by poor coating/substrate adhesion, extensive porosity, inter-splat oxidation and poor in-flight particle melting.

Porosity levels for Flame Spray coatings are generally reported to be 6-8%[13]. However, it can be seen in Table 5 that the coatings in this study had large variations in porosity levels, ranging from 2-40%. Coating porosity can develop from a number of sources[14], such as splat shrinkage during solidification, the presence of unmelted particles, entrapment of gas and, potentially, splat curl up. Although entrained gas can be difficult to eliminate, the in-flight melting characteristics of the particles is responsible for the other potential factors. Control

of the in-flight properties of the particles is related to the refinement of the parameters outlined in Table 2. In addition to these parameters, particle velocity and surface wettability have also been reported[15] as potential sources of porosity development. Therefore, by enhancing particle velocity, minimising exposure to oxygen and enhancing particle melting it should be possible to develop a Flame Spray coating with very low porosity(Table 2, R04). In addition, the substrate hardness can also affect the integrity of the deposited coating. Therefore, an understanding of the interaction between the deposition parameters, the substrate properties and the in-flight particles must be developed.

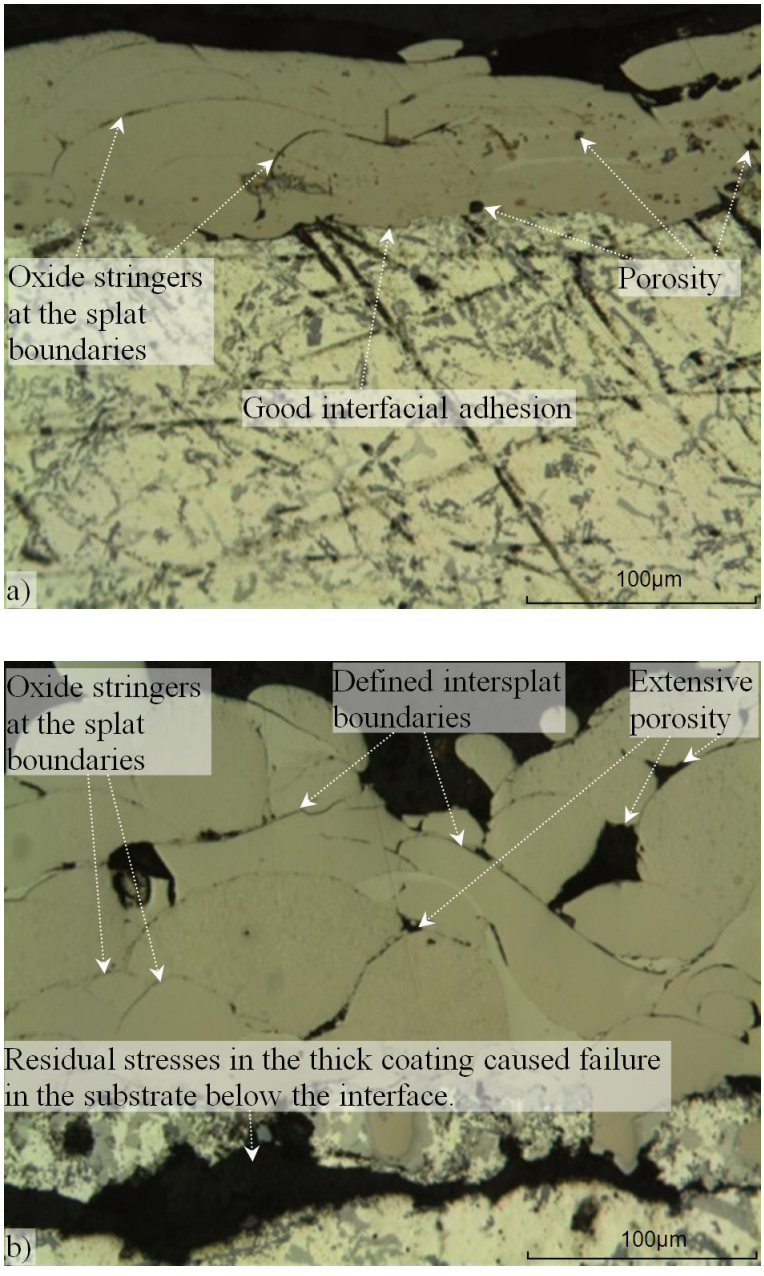

Figure 2 Photomicrographs of typical DOE NiCrBSi coatings showing variation in potential coating quality. a) LM25 (R10) b) LM24 (R15)

Run	Alloy			
	LM24		LM25	
	Porosity (%)	Coating Thickness (µm)	Porosity (%)	Coating Thickness (µm)
1	27.3	127.8	18.3	88.9
2	11.3	416.7	9.9	500.0
3	8.0	150.0	9.2	130.6
4	2.0	91.7	6.2	105.6
5	11.2	255.6	15.4	205.6
6	39.3	61.1	32.0	50.0
7	22.9	211.1	8.0	300.0
8	13.8	216.7	18.9	266.7
9	30.0	94.4	55.0	55.6
10	24.6	66.7	43.5	72.2
11	Samples delaminated		Samples delaminated	
12	4.8	125.0	9.6	122.2
13	5.5	1100	30.8	116.7
14	Samples delaminated		Samples delaminated	
15	11.6	611.1	12.8	233.3
16	10.7	172.2	13.7	155.6

Table 5 Table showing measured porosity levels and coating thicknesses for the NiCrBSi coatings on the cast Aluminium alloys.

As can be seen in Table 5, the deposited coatings exhibited strong dependencies on the deposition parameters, as large variations in both porosity and coating thickness were noted.

3.2 Taguchi Analysis

Figure 3, Figure 4 and Figure 5 outline the most important parameter interactions identified in this work. As can be seen, for the coatings on t he LM24 substrate, the strongest relationship appears to be between a powder flow rate, the nozzle type and the nozzle distance. Conversely, on the softer LM25 alloy, coating integrity appears to be unaffected by variations in the chosen parameters (Figure 5).

The analysis of the coatings on the LM24 alloy suggested that the key deposition parameters for controlling and minimising porosity were the distance between the nozzle and the work piece, the nozzle type and a potential interaction between the Gas Flow Rate(MFR_g) and the Powder Flow Rate(MFR_P). However, there appears to be no significant interaction between

the distance and the gas flow rate (Argon). Since the longer distance (300mm) produced lower porosity levels than the shorter distance (200mm), the hard LM24 surface appears to favour the impact of slower particles. And since coating integrity also improves at the higher powder flow rate, this combination of parameter settings may be related to the fundamental nature of the Thermal Spray processes.

In most Thermal Spray processes, molten particles impact the surface at high speed and plastically deform, forming a splat. However, if the particle temperature is too low when it reaches the surface, the effect would be similar to erosion wear[16], such as found in Warm spraying. Warm Spraying[17] operates at low temperatures producing reduced oxidation of the particles due to the lower application temperatures and superior coating properties have been noted[18]. Therefore it is suggested from these results that optimum coating properties, with respect to porosity levels, can be achieved by maintaining a distance of 300mm from the substrate surface, combined with either a high powder flow rate(3 $kg \cdot hr^{-1}$) and a low argon flow rate(9 nlpm) or a low powder flow rate(2 $kg \cdot hr^{-1}$) and a high argon flow rate(14 nlpm). From Table 2 the optimum coating setting would either be R04 or R06. From Table 5 R06 appeared to have very high porosity levels. Therefore it is suggested that the optimum parameters for the NiCrBSi coating onto the LM24 alloy would be R04.

Contrary to the results for the hard LM24 alloy, coatings on the softer LM25 substrate did not appear to respond as strongly to the parameters. While the shorter distance would seem to have provided a more coherent coating, the increased heat transfer to the aluminium alloy would require substantial additional cooling equipment.

Subsequent deposition work, based on the parameter settings for R04, confirmed the deposition of a coating with low porosity and a uniform coating thickness of 80-100µm (Figure 6).

3.3 Corrosion Analysis

Subsequent to the optimisation of the Flame Spray NiCrBSi coatings, coated samples were subjected to corrosion testing. Short-term corrosion testing was performed using Electrochemical Impedance Spectroscopy (EIS) in 0.1M NaCl solution. Results of this testing, for 6 hours immersion and 24 hours immersion, are shown in Figure 7.

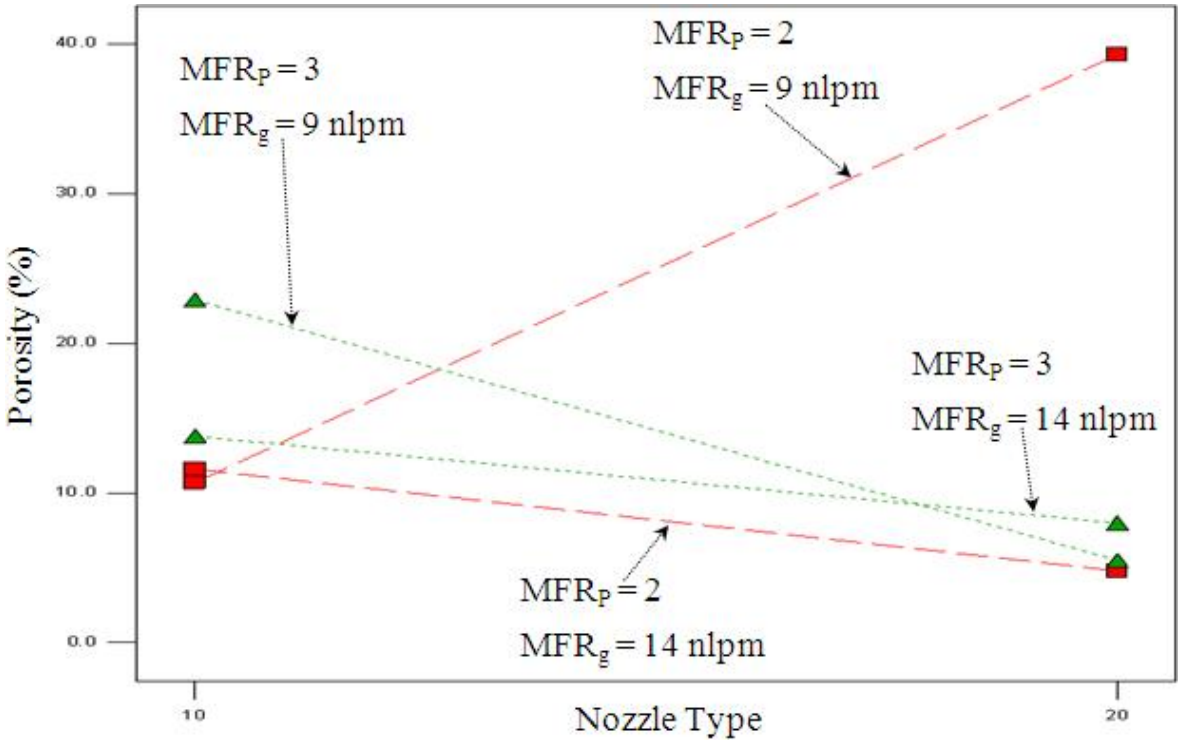

Figure 4 Effect of Interactions between Gas Flow Rate (MFRg), Powder Mass Flow Rate (MFRP) and Nozzle Type on the porosity levels in the deposited NiCrBSi coatings on LM24.

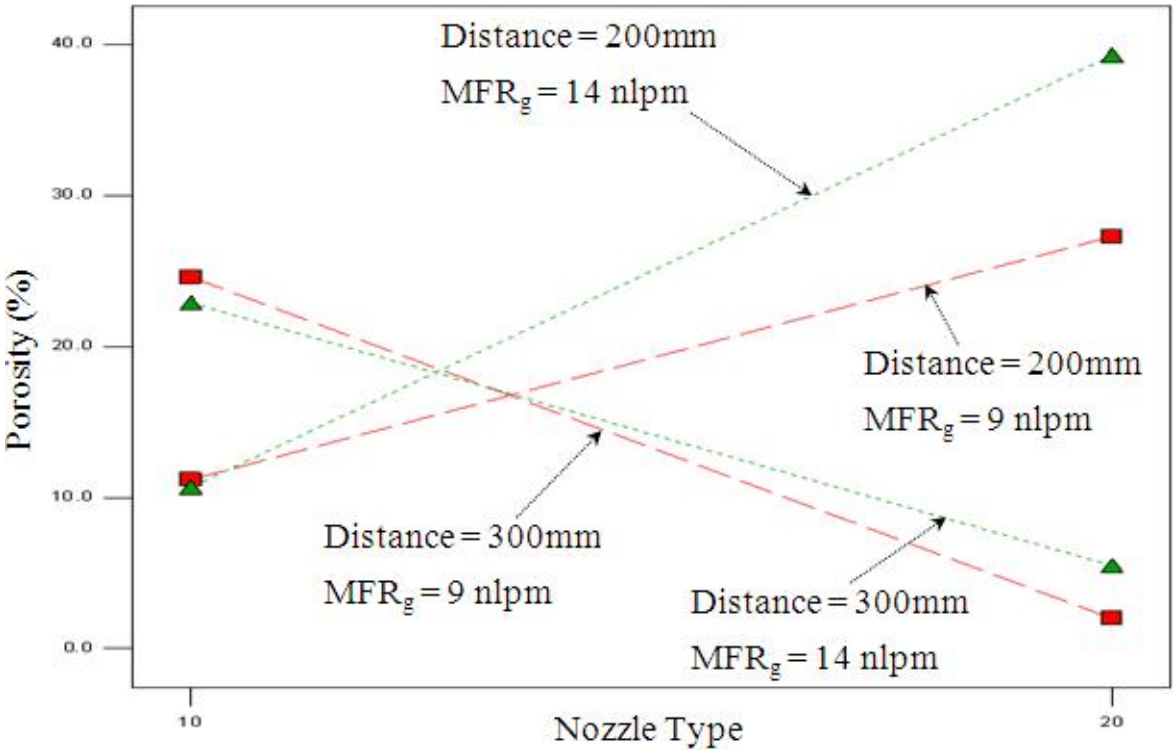

Figure 3 Effect of Interactions between Gass Flow Rate (MFRg), Nozzle Distance and Nozzle Type on the porosity levels in the deposited NiCrBSi coatings on LM24.

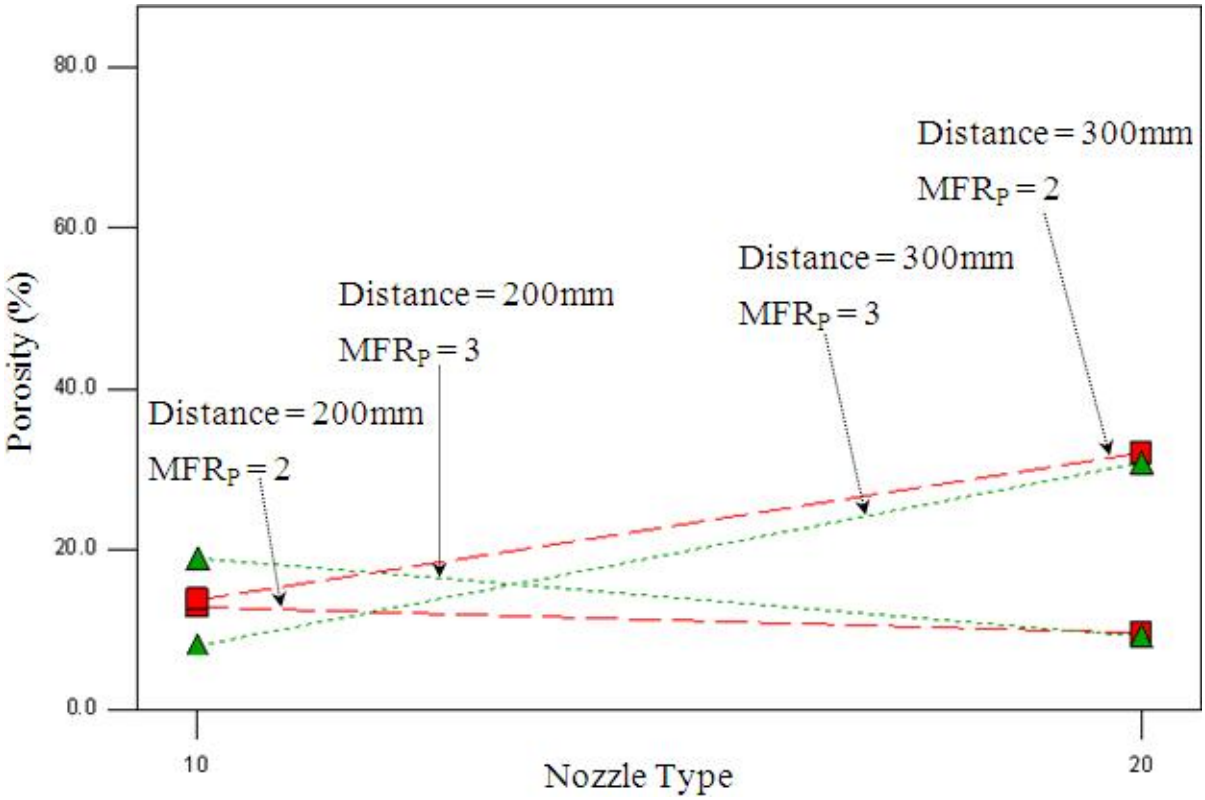

Figure 6 Effect of Interactions between Powder Flow Rate (MFR_P), Nozzle Distance and Nozzle Type on the porosity levels in the deposited NiCrBSi coatings on LM25.

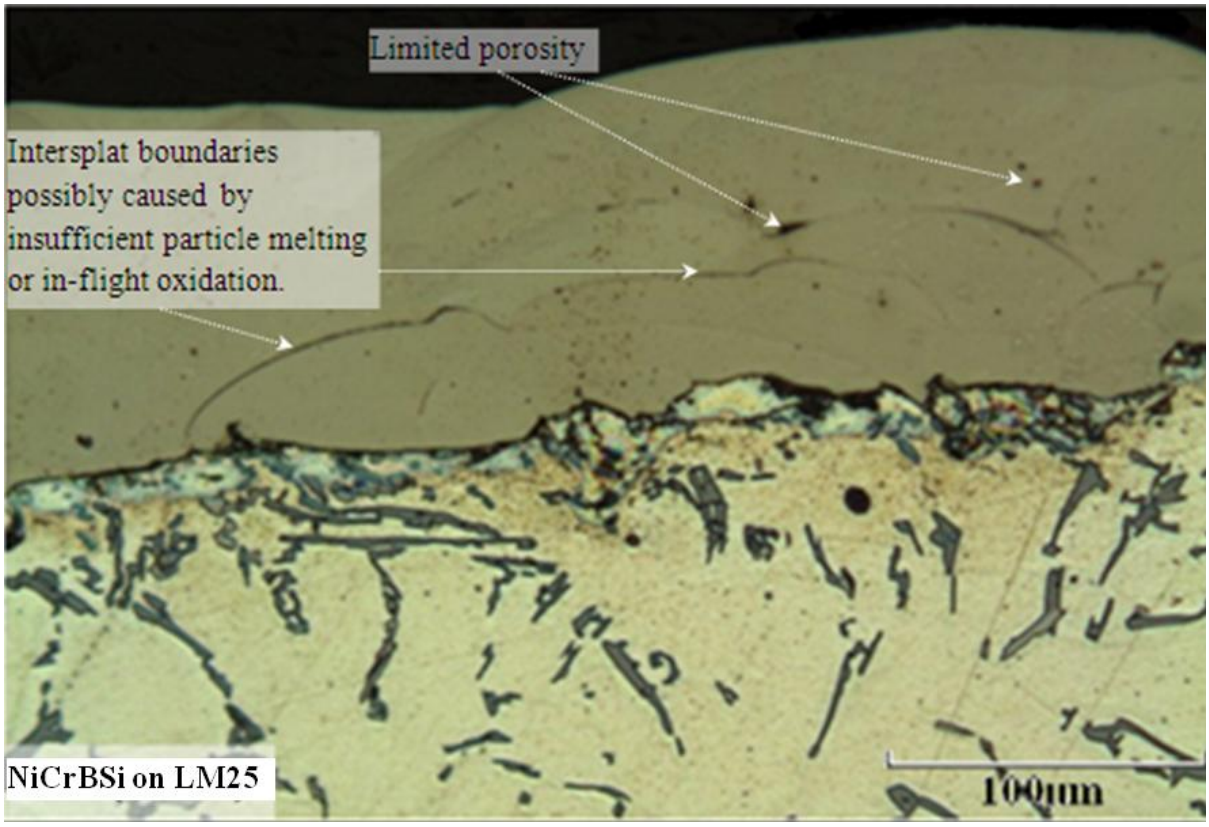

Figure 5 Optimised NiCrBSi Flame Spray coating on LM25.

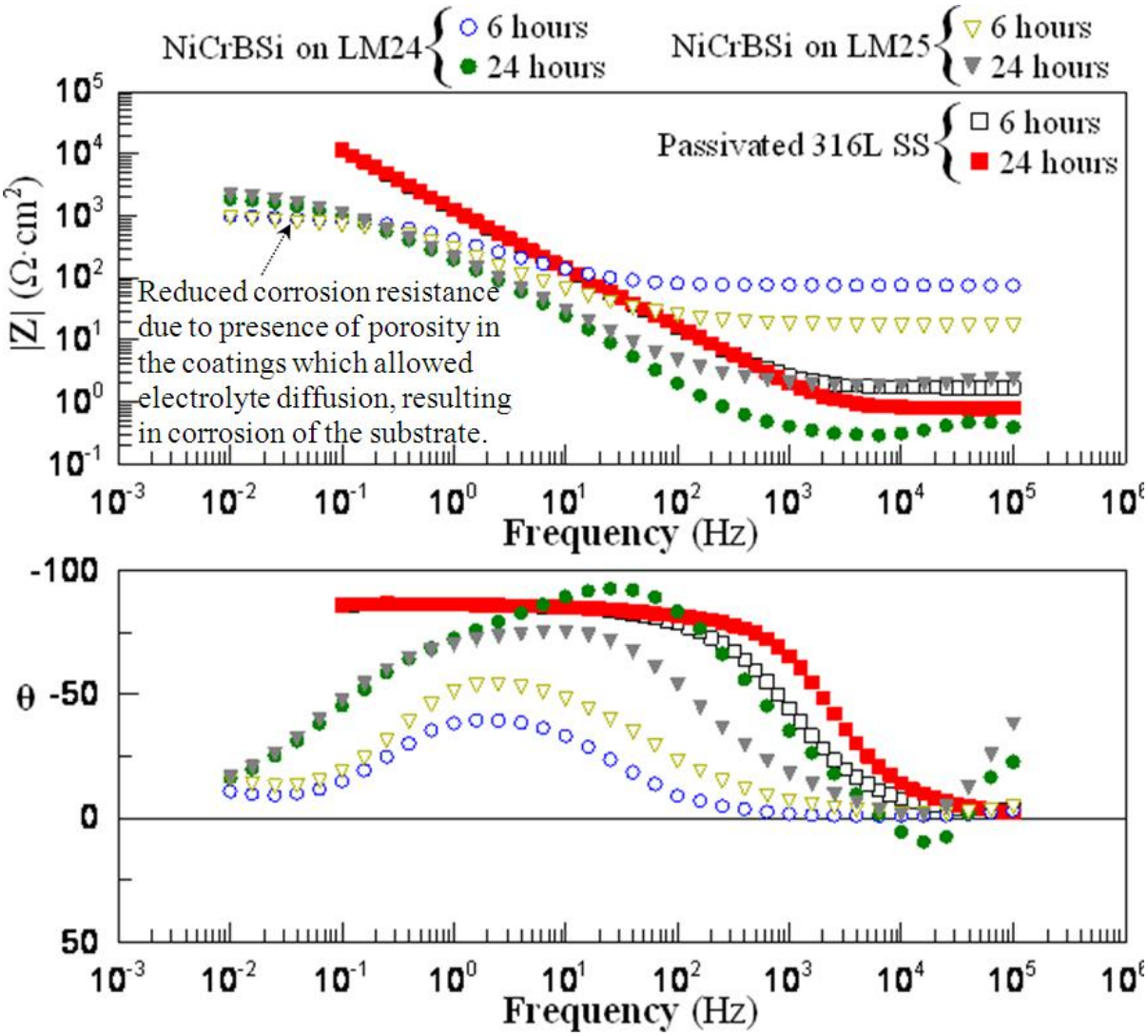

Figure 7 Bode Spectra (Impedance and Phase) for bulk 316L stainless steel and optimised NiCrBSi Flame Spray coatings on LM24 and LM25 in 0.1M NaCl solution.

The SS 316L substrate performed as expected in the corrosion tests, with no definable corrosion processes occurring during early immersion periods (0→24 hours). However, for the FS coatings, EIS performance levels were similar for both alloys. This would suggest substrate independent corrosion properties for these coatings. This is most likely attributable to the cathodic nature of these coatings, which, acted as large cathodic areas surrounding the active pores. Since there were equivalent coatings for both processes, the only quantifiable difference is the level of porosity in the coatings. The FS coatings had notably higher porosity levels than the equivalent HVOF coatings and this was reflected in the reduced R_p values for the FS coatings. In both instances, the rapid degradation of these systems in the presence of a corrosive agent resulted in spalling of the coating and exposure of nascent substrate material. Therefore porosity in the coatings became the primary failure conduit[19].

However, it is interesting to note that the corrosion of the coated systems appears to increase with increased immersion time.

In the corrosion of passivating metals, such as aluminium, pure activation control[20] does not exist and the corrosion processes can be either partially or primarily controlled by diffusion. In these instances, the polarisation resistance becomes primarily controlled by diffusion[21]. The time-dependent representation of the charge transfer process is also linked to the effusion of Al^{3+} ions into the electrolyte in the pore. Therefore the ability of the substrate to re-passify is fundamental to the corrosion resistance of the coated systems.

When an aluminium alloy is coated with a porous cathodic coating, such as in the work presented here, the development of the corrosion process is unlikely to be under pure activation control[22]. In this case, the development of corrosion process is dominated by two key processes[23] – Mass Transfer(MT) and Charge Transfer(CT). MT defines the anions at the electrolyte/metal interface and CT quantifies the oxidation/reduction reactions through electron exchange. High initial oxidation levels would rapidly expose the substrate to the corrosive environment and subsequent corrosion processes would be controlled by both CT and MT. As the corrosion process develops in the pores, however, the insoluble corrosion product interferes with the infusion of aggressive anions(Cl^-) and slows down the corrosion process. This can be seen to occur in Figure 6.

4 Summary

The process parameters for applying Flame Spray NiCrBSi coatings, as applied to two cast aluminium alloys (LM24 and Lm25) were studied. A Taguchi-based Design of Experiments approach was followed for optimising the coating deposition process. Four key parameters were identified and parameter settings were based on preliminary deposition work. Subsequent analysis of the deposited coatings was based on porosity measurements.

For the LM24 substrate, strong interactions were noted between all four of the selected process parameters. In general, low particle velocity and a narrower flame were detrimental to the integrity of the coating. However, this could be offset by increasing the flow-rate of the powder.

For the LM25 substrate, the parametric variations had little effect on the resultant deposited coatings.

Microstructural analysis of the optimised coatings indicated that substantial improvements had been achieved by performing the deposition optimisation work.

Corrosion testing of the coated substrates indicated that the coatings still contained porosity, as corrosion of the substrate was detected after only 1 hour immersion in 0.1M NaCl solution. However, the corrosion resistance of the coated substrate appeared to increase over the initial 24 hours immersion. This was attributed to pore blocking by the corrosion products which developed at the base of the pores.

5 References

[1] J. Stokes; *The Theory and Application of Sulzer Metco HVOF (High Velocity Oxy-Fuel) Thermal Spray Process* ©2008 Dublin City University

[2] J. Stokes, L. Looney; Surf. Coat. Technol. 148 (2001) 18-24

[3] J.M. Guilemany, J. Fernández, N. Espallargas, P.H. Suegama, A.V. Benedetti; Coat. Technol. 200 (2006) 3064-3072

[4] J. Kawakita, S. Kuroda, T. Fukushima, T. Kodama; Sci. Technol. Adv. Mater. 4 (2003) 281-289

[5] T.C. Hanson, G.S. Settles; J. Therm. Spray Technol. 12 (2003) 403-415

[6] T. Fukushima, S. Kuroda; Quart. J. Japan Weld. Soc. 20 (2002) 439-444

[7] S. Kuroda, J. Kawakit; ITSC (2004) 482-487

[8] D. Culliton, A. Betts, D. Kennedy; Int. J. Cast Metals 25 (2012) 9 pages

[9] S. Tobe; Proc. ITSC 15 (1998) 3-11

[10] V. Pershin, J. Mostaghimi, S. Chandra, T. Coyle; Proc. ITSC 15 (1998) 1305-1308

[11] M.F. Smith, D.T. McGuffin, J, A, Henfling, W. J. Lenling; J. Therm. Spray Technol. 2 (1993) 287-294

[12] O. Seri; Corr. Sci. 36 (1994) 1789

[13] S.V. Petrov, A.G. Saakov; Proc. EUROMAT'98 3 (1998) 105-113

[14] S. Safai, H. Herman; Thin Solid Films 45 (1997) 295-307

[15] H. Fukanuma; J. Therm. Spray Technol. 3 (1994) 33-44

[16] J.R. Davis; *Handbook of Thermal Spray Technology* ©2004 ASM International

[17] S. Kuroda, K. Kuroda; Sci. Technol. Adv. Mater. **9** (2008) 8 pges

[18] J. Kawakita, N. Maruyama, S. Kuroda, S. Hiromoto, A. Yamamiti; Mater. Trans. 49 (2008) 317-323

[19] M. Magnani, P.H. Suegama, N. Espallargas, S. Dosta, C.S. Fugivara, J.M. Guilemany, A.V. Benedetti; Surf. Coat. Technol. 202 (2008) 4746-4757

[20] R. Baboian; *Corrosion Tests And Standards: Application And Interpretation* © 2004 ASTM Int. 107-130

[21] M. Kuznecov, P. Otschik, P. Obenaus, K. Eichler, W. Schaffrath; Solid State Ionics 157 (2003) 371-378

[22] G. Kear, B.D. Barker, K. Stokes, F.C. Walsh; J. Appl. Electrochem. 34 (2004) 1235-1240

[23] Y.L. Cheng, Z. Zhang, F.H. Cao, J.F. Li, J. Q. Zhang, J.M. Wang, C.N. Cao; Corr. Sci. 46 (2004) 1649-1667